

Supporting Information

Hot-Electron Photodetector with Wavelength Selectivity in Near-Infrared via Tamm Plasmon

*Zhiyu Wang, J. Kenji Clark, Ya-Lun Ho, and Jean-Jacques Delaunay**

Department of Mechanical Engineering, School of Engineering, The University of
Tokyo, 7-3-1 Hongo, Bunkyo-ku, Tokyo 113-8656, Japan

*E-mail: jean@mech.t.u-tokyo.ac.jp

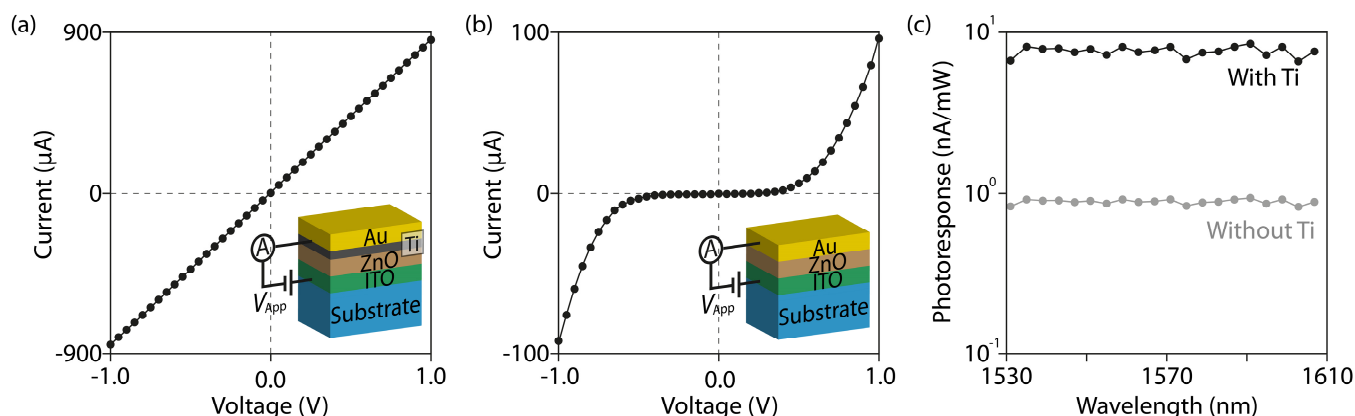


Fig. S1 Experimental results of I - V curves (S1a and S1b) and photoresponses (S1c) of the M-S-ITO structures with and without Ti thin film, with their schematic diagrams inserted. The two M-S-ITO structures were fabricated on fused quartz substrates. The ITO layer and ZnO layer in the two structures were deposited in a same process, and the Au films were deposited with same parameters. The thicknesses of the Au, Ti, ZnO, and ITO layers are 20 nm, 2 nm, 20 nm, and 20 nm, respectively. With the Ti thin film, the current versus voltage shows a linear relation indicating that both interfaces with the ZnO layer (i.e., Ti-ZnO and ZnO-ITO) form Ohmic contacts (Fig. S1a), while without the Ti thin film, a rectifying characteristic is preserved, indicating a Schottky contact forms at the Au-ZnO interface (Fig. S1b). The Schottky barrier height at the Au-ZnO interface is determined to be 0.71 eV using Cheung's functions^{S1} (with Richardson constant for ZnO of $32 \text{ A} \cdot \text{cm}^{-2} \cdot \text{K}^{-2}$, temperature of 295 K, contact area of 0.0025 cm^2 , and an ideality factor of 2.5). In contrast, the barrier height at the interface of Ti-ZnO is evaluated to be less than 0.35 eV, resulting in an one order larger photoresponse for the case with Ti thin film (as in Fig. S1c).

References

(S1) Cheung, S. K.; Cheung, N. W. Extraction of Schottky Diode Parameters from Forward Current-Voltage Characteristics. *Appl. Phys. Lett.* **1986**, *49*, 85-87.

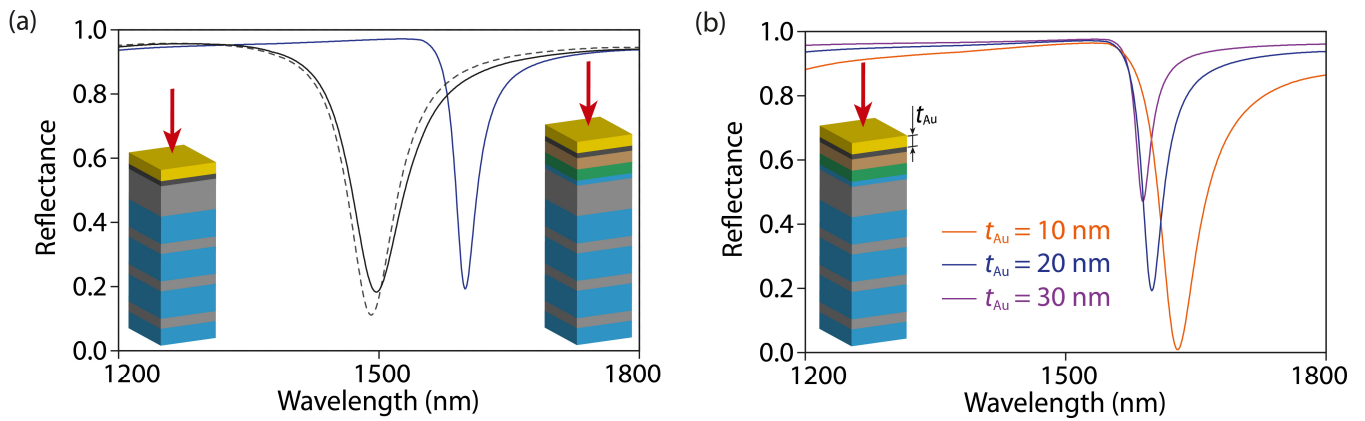


Fig. S2 (a) Simulated reflectance spectra of the TP structure with the 2-nm Ti film (black solid curve) and with all hot-electron device layers including the 10-nm insulation SiO₂, 20-nm ITO, 20-nm ZnO and 2-nm Ti layers (blue solid curve). The schematic diagrams are shown as the insets. The reflectance spectrum of the TP structure without all the additional layers (identical to the red curve in Fig. 2d) is also shown as reference (black dashed curve). (b) Reflectance spectra of the TP coupled hot-electron photodetector with different top Au thicknesses (t_{Au}). It is found that the thinner t_{Au} of 10 nm possesses a larger absorptance but a broader bandwidth of the resonance, whereas the thicker $t_{Au} = 30$ nm has a thinner line width but a weaker absorption.

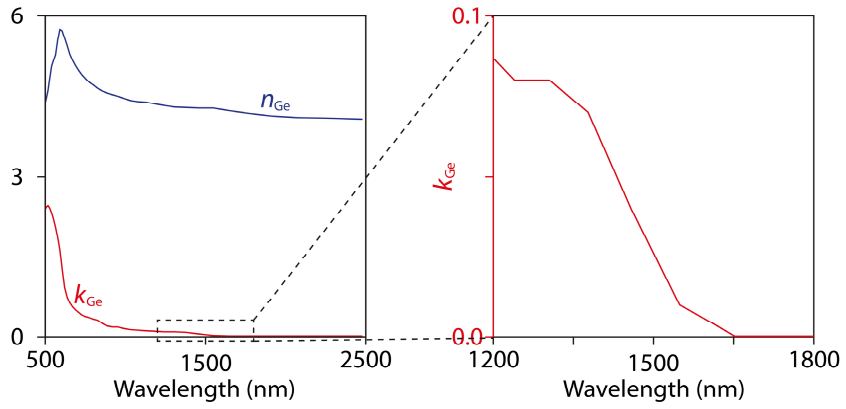


Fig.S3 Real part (n_{Ge}) and imaginary part (k_{Ge}) of refractive index of Ge as a function of wavelength (left), and the zoom-in view of the k_{Ge} in a range from 1200 nm to 1800 nm (right). As shown in the zoom-in view, k_{Ge} is nonzero at a wavelength around 1500 nm, and decreases for a longer wavelength.

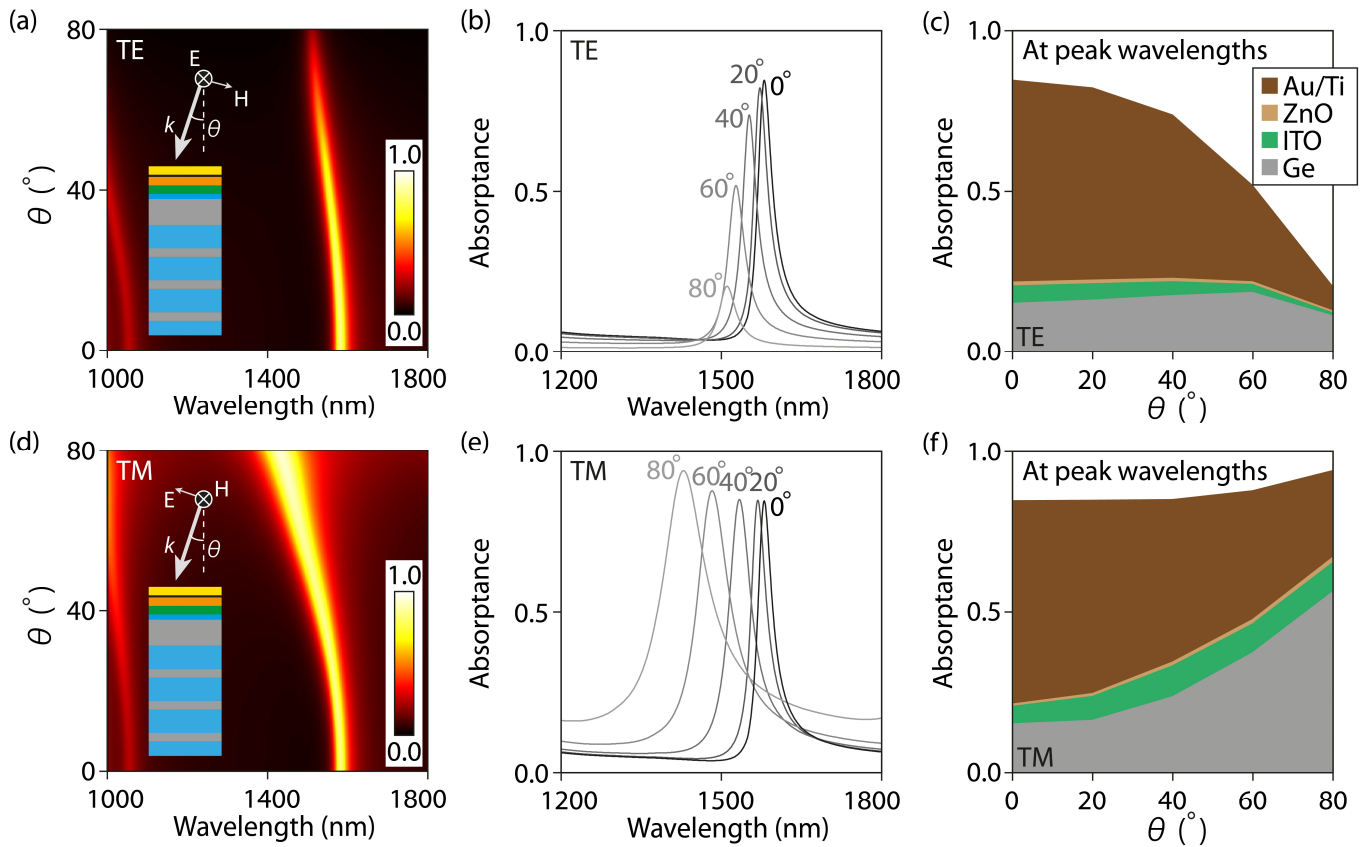


Fig. S4 Simulated optical behaviors of the fabricated TP hot-electron photodetector under oblique incidences for transverse-electric (TE) (a, b and c) and transverse-magnetic (TM) polarizations (d, e and f). Here, TE and TM polarizations are defined as the insets in (a and d). Both absorbance peaks for TE and TM exhibit a blue-shift as the incident angle increases. The absorbance at the peak wavelength for TE (TM) decreases (increases) with the incident angle. Fractions of light absorbed by the different materials in the device are also plotted in Fig. S4c and S4f. The incident angle dependent electrical photoresponse of this TP coupled hot-electron photodetector can be evaluated by the absorbance difference between the Au/Ti films (brown colored) and ITO film (green colored). Note that the enhancement of absorbance value with incident angle in TM case is mainly due to the increase in absorption in the Ge layers instead of the metallic layers. As a result, for both TE and TM, a weaker net photocurrent will be generated at larger incident angles (Fig. S4f).